

THERMAL ION FLOWS IN THE TOPSIDE AURORAL IONOSPHERE AND THE EFFECTS OF LOW-ALTITUDE, TRANSVERSE ACCELERATION

M. LOCKWOOD*

Radio Research Centre, Auckland University, Auckland, New Zealand

(Received in final form 13 January 1982)

Abstract—Topside ionospheric profiles are used to study the upward field-aligned flow of thermal O^+ at high latitudes. On the majority of the field lines outside the plasmasphere, the mean flux is approximately equal to the mean polar wind measured by spacecraft at greater altitudes. This is consistent with the theory of thermal light ion escape supported, via charge exchange, by upward O^+ flow at lower heights. Events of larger O^+ flow are detected at auroral latitudes and their occurrence is found to agree with that of transversely accelerated ions within the topside ionosphere and the magnetosphere. The effects of low altitude heating of O^+ by oxygen cyclotron waves, driven by downward field-aligned currents, are considered as a possible common cause of these two types of event.

1. INTRODUCTION

The populations of energetic O^+ ions which are found within the magnetosphere (see reviews by Prange, 1978; Johnson, 1979) indicate that an ionospheric source mechanism is active at auroral latitudes. The solar wind contains insufficient O^+ to act as the sole source and ions are observed to flow out of the topside ionosphere in upward-flowing ion (UFI) events (Ghielmetti *et al.*, 1978). These ions exhibit both field-aligned and conical pitch angle distributions and the morphologies of these "beams" and "conics" have been studied separately by Gorney *et al.* (1981). The beams are often inconsistent with a purely parallel acceleration acting below the satellite, neither can they all be explained as unresolved folded conics, mapped adiabatically from lower altitudes (Lysak *et al.*, 1980). The possible acceleration mechanisms have been reviewed by Mozer *et al.* (1980). There is a tendency for UFI events to be found within regions of field-aligned current, conics may be associated with currents of either sense, beams occurring mainly where they are upward (Cattell *et al.*, 1979). The composition of UFI's varies from nearly pure O^+ to nearly pure H^+ (Kintner *et al.*, 1979), the H^+ ions being recognised to be of ionospheric origin by their velocity space distributions (Croley *et al.*, 1978).

Observed fluxes within the magnetotail at $35R_E$ require an O^+ number flux of about $10^{12} \text{ m}^{-2} \text{ s}^{-1}$ to leave the topside auroral ionosphere (Frank *et al.*, 1977), a figure which is consistent with observations made below $1R_E$ (Klumpar, 1979). The continuous polar wind outflow of cold ionospheric plasma persists along all field lines at latitudes higher than the outer plasmasphere with total fluxes of the order of $10^{12} \text{ m}^{-2} \text{ s}^{-1}$ (Hoffman and Dodson, 1980). Hence if the polar wind is to act as a source of O^+ for the magnetosphere it must, on occasions, consist of nearly pure O^+ at certain auroral latitudes. The theory of thermal plasma escape predicts that less than 10^{-3} of the total polar wind is O^+ (Banks and Holzer, 1969), the thermal O^+ escape being restricted to such low fluxes by an effective barrier presented by charge exchange with neutral hydrogen. Thus thermal escape, with subsequent heating at greater altitudes, is an insufficient source of O^+ for the magnetosphere by a factor of at least one thousand.

Moore (1980) has extended polar wind theory to allow for the presence of either parallel or transverse ion heating at low altitudes. The effect of such an acceleration is to reduce the charge exchange cross section, thereby allowing supra-thermal ions to escape into the magnetosphere. Moore found that the threshold heating rate for O^+ escape due to parallel acceleration is very low, provided that the forcing is continued. For transverse acceleration about 10 eV must be imparted

*Present address: Rutherford Appleton Laboratory, Chilton, Didcot, Oxon. OX11 0QX, U.K.

to the ion, which is subsequently moved upward by the gradient B force and is "mirrored" out of the ionosphere. The observed variability of the upward-flowing O^+ is then explained by variations in the height of the acceleration region, relative to the O/H neutral transition altitude.

The S3-3 observations of UFI events reported by Ghielmetti *et al.* (1978) were made using the satellite's ion mass spectrometer, which detects energies between 0.5 and 16 keV and affords resolution of the different ion species. Also on board S3-3 is an electrostatic analyser (ESA) which can detect energies as low as 90 eV, but has no mass resolution. Ghielmetti *et al.* (1978) found only one UFI event below 5000 km, indicating the main acceleration region is too high to be a cause of O^+ escape. However, the ESA data shows that although ions are heated strongly near 5000 km, taking them above the detection threshold of the ion mass spectrometer for the first time, there is some heating at lower altitudes to lower energies (Kintner *et al.*, 1979). A full study of the ESA data by Gorney *et al.* (1981) has shown that although beams are mainly found above 5000 km low energy conics (< 0.4 keV) are found at much lower altitudes. During disturbed times the frequency of observation of such conics actually increases with decreasing altitude below 2000 km. Observations from both ISIS satellites also reveal transversely accelerated ions in the ionosphere (Ungstrup *et al.*, 1979; Klumpar, 1979) as do data from AE-C (Brinton and Grebowky, 1978, unpublished results) and various rocket flights (Bering *et al.*, 1975; Whalen *et al.*, 1978).

Transverse heating of ions may result from either resonant wave-particle interactions, or from spatially-confined, quasi-static D.C. electric fields (Mozer *et al.*, 1980). The two types of wave which are most likely to be involved are electrostatic ion cyclotron waves (EIC) and lower hybrid resonance waves.

The observed correlation between EIC waves and UFI events (Kintner *et al.*, 1979; Ungstrup *et al.*, 1979) indicates that either these waves are driven by the suprathermal ions or that they are responsible for at least part of the ion's heating. Kindel and Kennel (1971) showed that EIC waves are unstable to the field-aligned currents found within the auroral zone, the instability occurring at lower altitudes when the current density is larger. The association of conics with field-aligned currents (Cattell *et al.*, 1979; Cattell, 1981) implies that perpendicular ion heating may be caused by EIC waves driven by field-aligned currents. The strong

ion heating near 5000 km, inferred from the S3-3 data, has been considered theoretically by a number of authors. Palmadesso *et al.* (1974) considered heating by random-phase EIC turbulence and Papadopoulos *et al.* (1980) have shown that hydrogen cyclotron waves can preferentially accelerate O^+ ions, when they are present as a minor constituent. This stochastic process, however, is effective when the O^+ ions are already pre-heated at lower altitudes. The S3-3 plasma wave receiver detects some EIC waves with long coherence times (Mozer *et al.*, 1980) and heating by such "strong" EIC turbulence has been considered by Lysak *et al.* (1980) and the theory contrasted with the random-phase, quasi-linear theory of Palmadesso *et al.*

Waves at the low hybrid resonance are found throughout the auroral zone (Mozer *et al.*, 1980). Transversely accelerated ions were associated with VLF emissions by Klumpar (1979) and hence may be due to lower hybrid waves. However, it is thought that such waves may be responsible for further heating of a hot tail of the energy spectrum, particularly for the case of O^+ ions (Mozer *et al.*, 1980; Lysak *et al.*, 1980).

A third mechanism by which O^+ ions may be heated involves regions of perpendicular, quasi-static, spatially-confined DC electric field. If the gyroradius of the ion motion is much greater than the width of such a region, transverse heating can result. This condition is more easily met for O^+ than for H^+ , and for ions of higher initial energy (Lysak *et al.*, 1980; Mozer *et al.*, 1980).

The three mechanisms for transverse acceleration of O^+ described above (due to hydrogen cyclotron waves, lower hybrid waves and quasi-static DC electric fields) are all most efficient for ions of elevated energy. Hence, although they may be responsible for the ultimate energy which O^+ ions achieve at great altitudes, none of them is likely to be the process which initially heats them above thermal, and hence causes escape of ionospheric O^+ , even if they were active at sufficiently low altitudes. Ashour-Abdalla *et al.* (1981) have modelled O^+ heating by oxygen cyclotron waves for the ion transition altitude in the topside ionosphere, where O^+ and H^+ densities are equal. The group velocity of the ion cyclotron waves is much smaller than the electron drift speed, allowing electrons to supply free energy continuously. In this case the hydrogen cyclotron wave saturates, following which oxygen cyclotron waves grow and transversely accelerate the O^+ . The heating rates predicted by this model are

large, provided the free energy source is present for sufficient time. Ashour-Abdalla *et al.* predict oxygen cyclotron waves should be present in the auroral topside ionosphere, however they remain difficult to detect. Bering *et al.* (1975) observed turbulence close to the O^+ gyrofrequency during a rocket flight. Satellite observations of such low frequency turbulence cannot be unambiguously identified as being due to oxygen cyclotron waves because of the large Doppler shifts.

Lockwood and Titheridge (1981) observed upward flows of thermal O^+ ions near the poleward edge of the nocturnal auroral oval with mean values for equinox conditions $0.35 \times 10^{13} \text{ m}^{-2} \text{ s}^{-1}$ when $K_p < 2$ and $0.75 \times 10^{13} \text{ m}^{-2} \text{ s}^{-1}$ when $K_p \geq 2$. These fluxes are significantly larger than the corresponding values for the remainder of the polar cap of $0.1 \times 10^{13} \text{ m}^{-2} \text{ s}^{-1}$ and $0.2 \times 10^{13} \text{ m}^{-2} \text{ s}^{-1}$, respectively, and the value of $0.1 \times 10^{13} \text{ m}^{-2} \text{ s}^{-1}$ for the light ion polar wind observed at 1400 km when $K_p < 2$. These latter fluxes are deduced from the roll modulation of ISIS 2 ion mass spectrometer data by Hoffman and Dodson (1980). Under steady state conditions the flux observed by Lockwood and Titheridge (1981) should, by continuity, equal the total ion outflow; these results together imply the presence of either large-scale transient filling of the topside ionosphere between 500 and 1400 km, or of some additional mechanism of ion escape into the magnetosphere. The results of Hoffman and Dodson are based on the assumption that there is no O^+ flow at 1400 km, the light ion velocities being deduced from the phase shift in the roll modulation for that species, relative to that for O^+ . Hence, the ISIS 2 results do not include any information on O^+ flows; there is however little or no reduction in the light ion flow at 1400 km at auroral latitudes. Hence, any upward O^+ outflow, which would remain undetected, would require an enhanced O^+ flux at lower altitudes, a feature which is evident in the results of Lockwood and Titheridge (1981).

Transient filling of the topside ionosphere has been modelled by Whitteker (1977) who studied the response of the topside O^+ density profile to the onset of soft electron precipitation. This onset may correspond to a sharp increase in the number of precipitating particles or to the convection of plasma into a region where such precipitation is present. The response of the topside plasma to this stimulus is an acceleration of O^+ ions upward, forming a bulge in the O^+ density profile which moves rapidly upward, reaching 1000 km within about 5 min and 2000 km 10 min later.

In this paper profiles exhibiting the behaviour modelled by Whitteker are removed from the data set, eliminating the effects of transient filling of the topside ionosphere below the satellite. The latitudinal, local time, magnetic activity and seasonal variations of remaining events of large upward thermal ion flow are then compared with those of UFI events.

2. OBSERVATIONS

The database employed comprises 60,000 scale height profiles, as observed between 1962 and 1968 by the topside sounder on board the Alouette 1 satellite, and is the same as that in the previous work by Lockwood and Titheridge (1981). The analysis in that study was restricted to equinox conditions because only then were sufficient observations available to construct the variation of the mean flux with latitude; here solstice observations are investigated by looking for events of large upward O^+ flow. The numbers of satellite passes analysed for each month are as given by Titheridge (1976). Due to the lack of telemetry stations for the southern polar cap only northern hemisphere data were used. Successive soundings were averaged together to smooth out the effects of experimental error and of transient phenomena such as travelling ionospheric disturbances. The number of soundings in each grouping was usually six, and was chosen such that each grouping spanned about five degrees of latitude; hence smoothing is achieved at the expense of spatial resolution. The UFI events observed by various other satellites vary in latitudinal width from a fraction of a degree (when accelerated ions are seen only for a few successive spacecraft spins) up to about 8° (Ghielmetti *et al.*, 1978). The necessary averaging of soundings will weigh this study in favour of detecting the effects of such events with greater latitudinal width. The scale height profiles extend from the satellite at 1000 km down to about 400 km, and observations of the O^+ flux are made in the range 500–600 km (for reasons outlined by Lockwood and Titheridge, 1982).

The plasma density profile shown in Fig. 1(a) is an example of a type of profile found occasionally in the data set employed by Lockwood and Titheridge (1981) and which is of a form modelled by Whitteker (1977). The signature in the corresponding scale height profile, shown in Fig. 1(b), would be detected for all cases when the bulge in the O^+ density was below 1000 km, which is equivalent in the model of Whitteker to cases within about 5 min of the onset of particle precipitation. As the

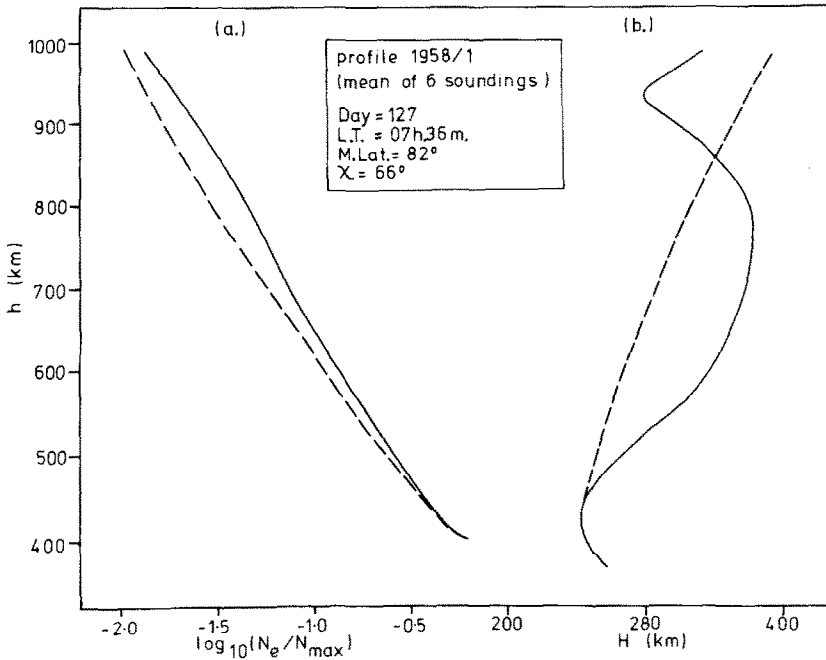


FIG. 1. EXAMPLE OF SMOOTHED OBSERVED PROFILES INDICATING UPWARD ION FLOW GIVING TOPSIDE FILLING BENEATH THE SATELLITE (a) PLASMA DENSITY PROFILE (b) THE EQUIVALENT PLASMA SCALE HEIGHT PROFILE.

Dashed curves are diffusive equilibrium model profiles for comparison.

bulge moves upward the height of peak upward flow increases and the flow in the 500–600 km range decreases after 5 mins even if the precipitation persists; if it ceases the flow becomes downward rapidly. Hence, removing all cases from the data set which show the signature demonstrated by Fig. 1(b) eliminates cases showing filling of the topside ionosphere due to particle precipitation, except those for which precipitation is still present and has been so for in excess of 5 min following a sudden onset. For these latter cases the filling and peak upward flow are occurring above the sounder and a large upward ion flow would also be observed at 1400 km, the altitude of the ISIS 2 ion mass spectrometer.

Each of the 10,000 averaged scale height profiles was inspected visually and all cases of the form of Fig. 1(b) were eliminated. The remaining data subset consists of 1568 mean profiles obtained within 50 days of the equinoxes in the years 1962–1968 at geomagnetic latitudes greater than 50°. The corresponding numbers for similar 100 day periods centred on the summer and winter solstices were 570 and 827, respectively.

A flow of O^+ ions, relative to the neutral atmosphere, affects the shape of the topside profile

only where the ion–neutral frictional drag is large. This effect is illustrated by the steady-state, theoretical plasma scale height profiles, $H(h)$, shown in Fig. 2. These are derived using an adap-

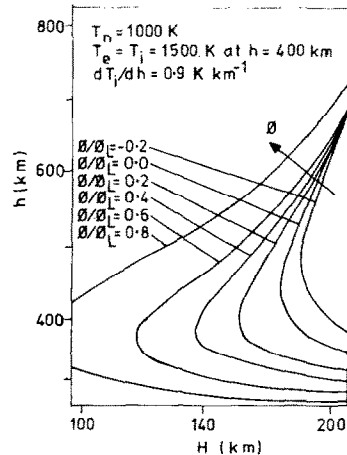


FIG. 2. MODEL, STEADY-STATE, SCALE HEIGHT PROFILES, $H(h)$, FOR VARIOUS O^+ ION FLUXES, θ , EXPRESSED AS A FRACTION OF THE LIMITING VALUE SET BY ION-NEUTRAL FRICTIONAL DRAG, θ_L .

After Lockwood and Titheridge (1981).

tation of the model by Titheridge (1976) for various values of the O^+ ion flux, ϕ , expressed as a fraction of its limiting value, ϕ_L (Lockwood and Titheridge, 1982). The neutral temperature, T_n , and the plasma temperature gradient, dT_p/dh , are independent of height in this example, and equal to 1000 K and 0.9 K km^{-1} , respectively; the plasma temperature at 400 km is 1500 K. The height of the F2 peak varies between 300 km for diffusive equilibrium ($\phi = 0$) and about 275 km for (ϕ/ϕ_L) equal to 0.8. Just above the F2 peak H is reduced by an upward flux of O^+ ions. Because this effect is due to ion-neutral frictional drag, it is desirable to define ϕ as:

$$\phi = N_{o+}(V_n - U_n) \quad (1)$$

where N_{o+} is the O^+ density and V_n and U_n are the upward field-aligned velocities of O^+ ions and neutral atoms, respectively. At greater altitudes the lower neutral densities cause frictional drag to be small and H becomes independent of ϕ . Figure 3 shows an observed profile exhibiting the kind of deviation modelled in Fig. 2, the dashed profile being an extrapolation based on diffusive equilibrium under the same temperature and com-

position conditions. Lockwood and Titheridge (1982) have used model profiles, of the kind shown in Fig. 2, to calibrate the deviation of $H(h)$ as a function of (ϕ/ϕ_L) , over a wide range of conditions. The accuracy of this calibration was checked by comparing the values deduced from other model profiles with the values used to generate them. Overall it was found that (ϕ/ϕ_L) could be determined from an observed profile to within an accuracy of 2%, the principle error arising from the experimental uncertainty in H at the altitude of observation, well below the satellite.

The absolute magnitude of the ion flux, ϕ , can also be evaluated for each averaged sounding using the method described by Lockwood (1982). Briefly, a model diffusive-equilibrium scale height profile, fitted to the observed $H(h)$ profile using the procedure of Titheridge (1976), is corrected to allow for the effects of ion flow using the known value of ϕ/ϕ_L . This gives the true diffusive-equilibrium scale height, H_0 , shown as the dotted extrapolations in Figs. 1 and 3. A set of equations is then solved iteratively giving ϕ from the difference $(H_0 - H)$, the values for the plasma density, temperature and temperature gradient (taken from the sounding using the method of

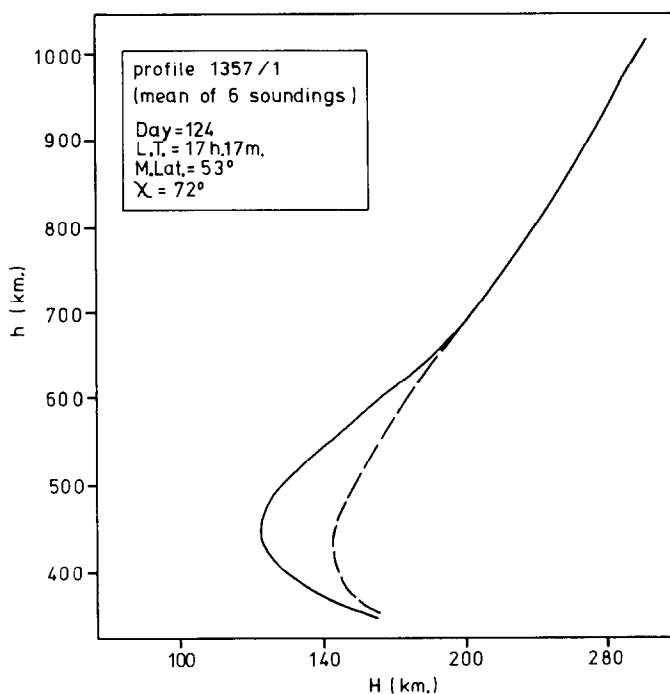


FIG. 3. EXAMPLE OF A SMOOTHED OBSERVED SCALE HEIGHT PROFILE EXHIBITING THE EFFECTS OF ION FLOW.

The dashed curve is an extrapolation for diffusive equilibrium conditions.

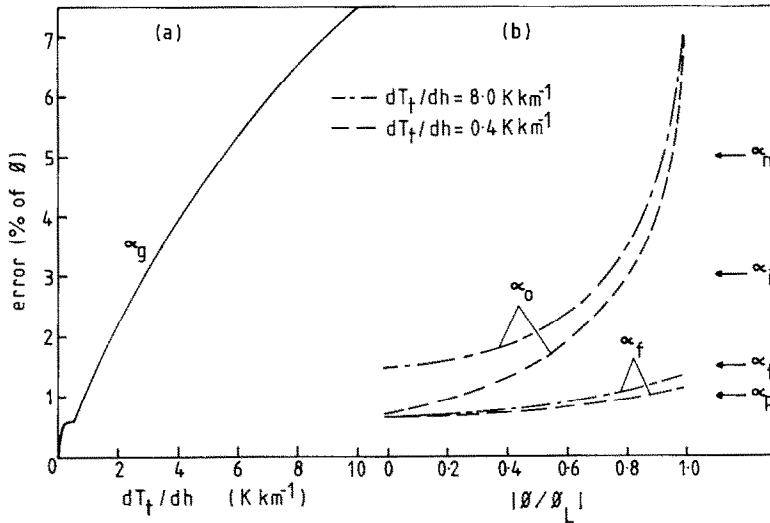


FIG. 4. MAXIMUM ERRORS IN UPWARD FLUX VALUES, AS A PERCENTAGE OF θ : (a) DUE TO dT_p/dh , THE PLASMA TEMPERATURE GRADIENT, α_g ; (b) DUE TO THE SCALE HEIGHTS H_o AND H , α_o AND α_f RESPECTIVELY, FOR dT_p/dh OF 0.4 AND 8.0 K km^{-1} .

On the right are shown errors α_n , α_o , α_i and α_p ; due to uncertainties in neutral oxygen density and temperature and ion temperature and density respectively.

Titheridge, 1976) and estimates of the neutral temperature, composition and density (taken from the MSIS neutral atmospheric model). The use of mean statistical model values for neutral atmosphere parameters introduces larger errors into the deduced value of θ than in θ/θ_L . Figure 4 summarises the results of an analysis of the maximum errors in the value of θ deduced by this procedure due to the uncertainties in the various parameters used (Lockwood, 1982). The largest error is almost always α_n , due to the uncertainty of the MSIS neutral oxygen density prediction; the plasma temperature gradient can introduce a larger error

only in the rare event of it exceeding 6 K km^{-1} and errors in the value of H_o cause larger errors only when θ/θ_L exceeds 0.9, never observed in the study by Lockwood and Titheridge (1982). Figure 4 gives maximum estimates of the component errors in θ , the total error in each value is typically between 5 and 10%.

3. RESULTS

3.1. Mean upward flows within the polar cap and large upward flux events

The points in Fig. 5 show mean values of θ and θ/θ_L in various K_p bins for equinox observations

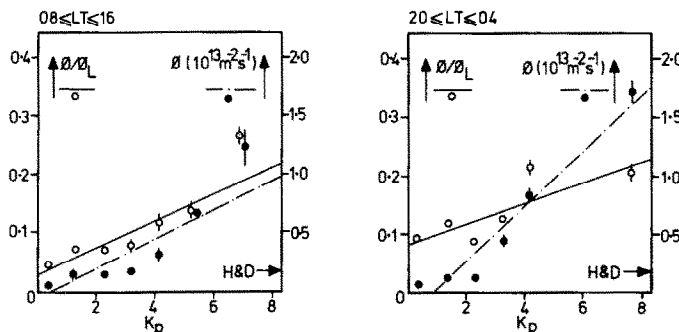


FIG. 5. MEAN VALUES OF θ (SOLID POINTS) AND θ/θ_L (OPEN POINTS) IN VARIOUS K_p BINS WITH ERROR BARS OF ONE STANDARD ERROR IN THE MEAN.

Linear regression lines are shown as broken and full lines for θ and θ/θ_L , respectively. Means are for all observations poleward of the statistical auroral and in local time ranges 08–16 h (left) and 20–04 h (right). The flux marked H and D is the mean light ion flow observed at 1400 km for $K_p < 2_o$ by Hoffman and Dodson (1980).

taken within the polar cap. The boundary of the polar cap is taken to be the poleward edge of the statistical auroral oval predicted for the magnetic activity at the time of each sounding (as done in Lockwood and Titheridge, 1981). The error bars are plus and minus one standard error in the mean, due to the spread of the individual values, and are generally similar in magnitude to the experimental uncertainty of each value. Figure 5(a) is for observations taken within 4 h of local midday and Fig. 5(b) is for those within 4 h of midnight. The values marked "H and D" show the means of the light ion flux observed by ISIS 2 at these times and latitudes, for observations when the K_p value was less than 2_o , there being little variation about this mean across the entire polar cap. All flux values are normalised to a height of 1000 km. The mean light ion flow observed for K_p less than 2_o from ISIS 2 data is approximately equal to the values of θ at all K_p less than 3_o . This is consistent with the theory of steady-state thermal polar wind escape, where the light ion flux is supported by an upward flow of O^+ at lower altitudes (Banks and Holzer, 1969). At K_p greater than 3_o the values of θ increase, giving the observed slope to the regression (dashed) lines. Without similar data on the light ion flow at these higher magnetic activities, it is not known if this constitutes a departure from the theory.

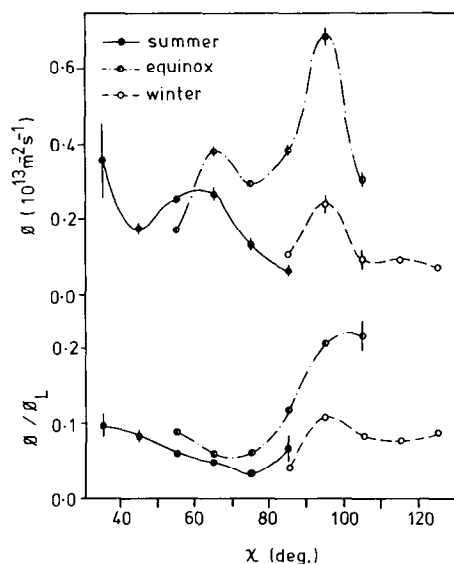


FIG. 6. MEAN VALUES OF θ AND θ/θ_L AS A FUNCTION OF SOLAR ZENITH ANGLE, χ , FOR OBSERVATIONS POLEWARD OF THE STATISTICAL AURORAL OVAL WITHIN 50 DAYS OF SUMMER AND WINTER SOLSTICES AND THE EQUINOXES, WITH ERROR BARS OF ONE STANDARD ERROR IN THE MEAN.

There are ion-dynamic effects associated with plasma convecting into the sunlit hemisphere. This is shown by Fig. 6, plots of mean values of θ and θ/θ_L in 10° bins of solar zenith angle, χ , for summer, winter and equinox observations within the polar cap. There are peaks near 100° , indicating upward flows near the terminator of the light and dark hemispheres.

The large mean values of θ found near the poleward edge of the auroral oval by Lockwood and Titheridge (1981) have large standard deviations. Closer inspection of the data shows that values of θ at these latitudes fall into two categories: values which, allowing for errors in the MSIS model, could be attributed to light ion polar wind flux (below $0.5 \times 10^{13} \text{ m}^{-2} \text{ s}^{-1}$) and frequent "events" of larger values of θ . These events are defined here as when θ exceeds $0.75 \times 10^{13} \text{ m}^{-2} \text{ s}^{-1}$ and χ does not fall in the range 90 – 110° , ensuring that any contributions by layer sunrise effects (as shown in Fig. 6) are eliminated.

3.2. Morphology of large upward flow events

The local time–geomagnetic latitude plots in Figs. 7–10 show the locations where the smoothed profile gives a value of θ in certain ranges greater than $0.75 \times 10^{13} \text{ m}^{-2} \text{ s}^{-1}$. Figure 7 is for observations taken within 50 days of a winter solstice, and Fig. 8 is for those in a similar period around the summer solstice. In both cases these large values of θ are present in the lower latitudes of the polar cap and in the poleward half of the auroral oval. However, in summer they are relatively rare and those that are found are clustered around the cleft, whereas during winter they cover a range of local times on the nightside, between 18 and 09 L.T. That these events are associated with the auroral oval is demonstrated by Figs. 9 and 10, which combine the summer and winter events shown in Figs. 7 and 8, for when $K_p < 2_o$ and $K_p \geq 2_o$, respectively. The locations of these events at times of higher activity are generally at lower latitudes, the local time variation being characteristic of the auroral oval in both cases.

The results of Figs. 7–10 may show some bias due to incomplete satellite coverage, a problem aggravated by the elimination of all profiles exhibiting refilling of the topside ionosphere below the satellite and of those for which χ is between 90 and 110° . There are fewer profiles available for analysis near the magnetic pole, and this may be the cause of the small number of events at the centre of the polar cap. Figure 11 gives the occurrence probabilities of large flux events, defined as

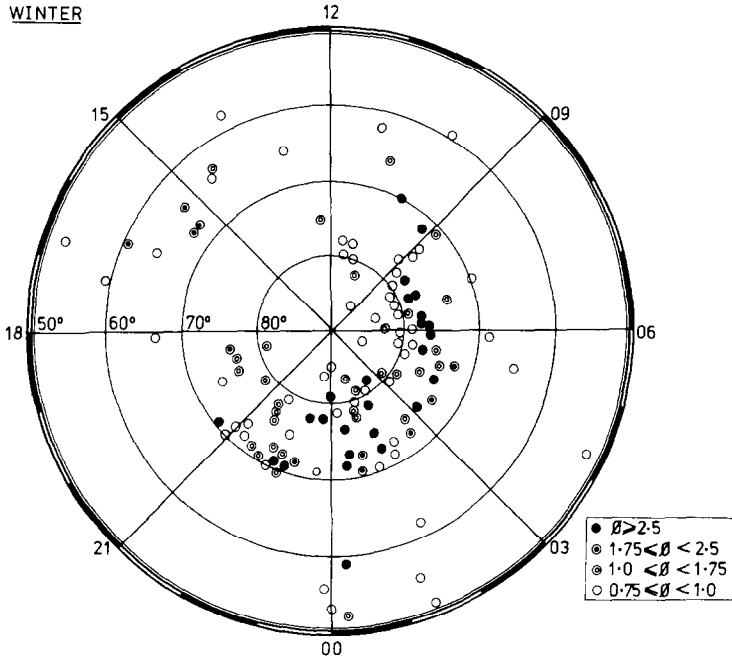


FIG. 7. LOCAL TIME-GEOMAGNETIC LATITUDE PLOT OF OBSERVATIONS OF θ IN VARIOUS RANGES (IN $10^{13} \text{ m}^2 \text{ s}^{-1}$) WITHIN 50 DAYS OF A WINTER SOLSTICE.

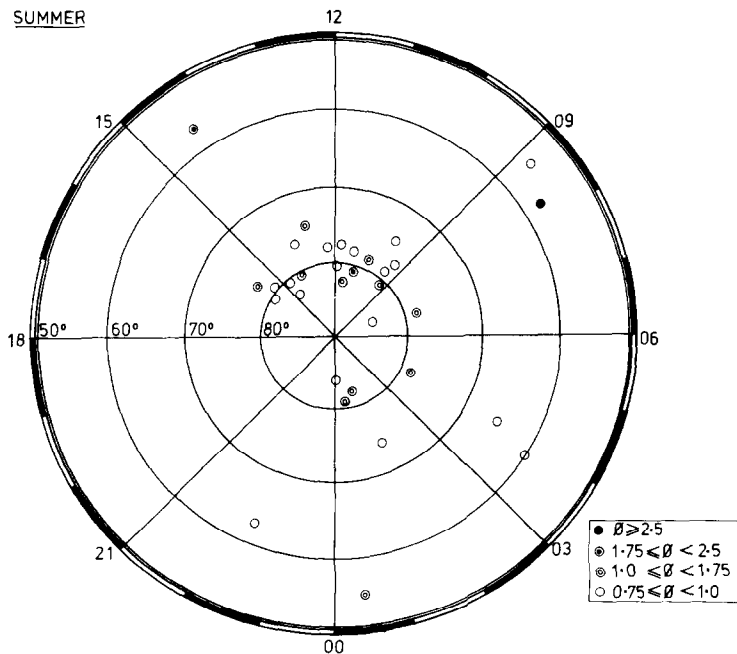


FIG. 8. LOCAL TIME-GEOMAGNETIC LATITUDE PLOT OF OBSERVATIONS OF θ IN VARIOUS RANGES (IN $10^{13} \text{ m}^2 \text{ s}^{-1}$) WITHIN 50 DAYS OF A SUMMER SOLSTICE.

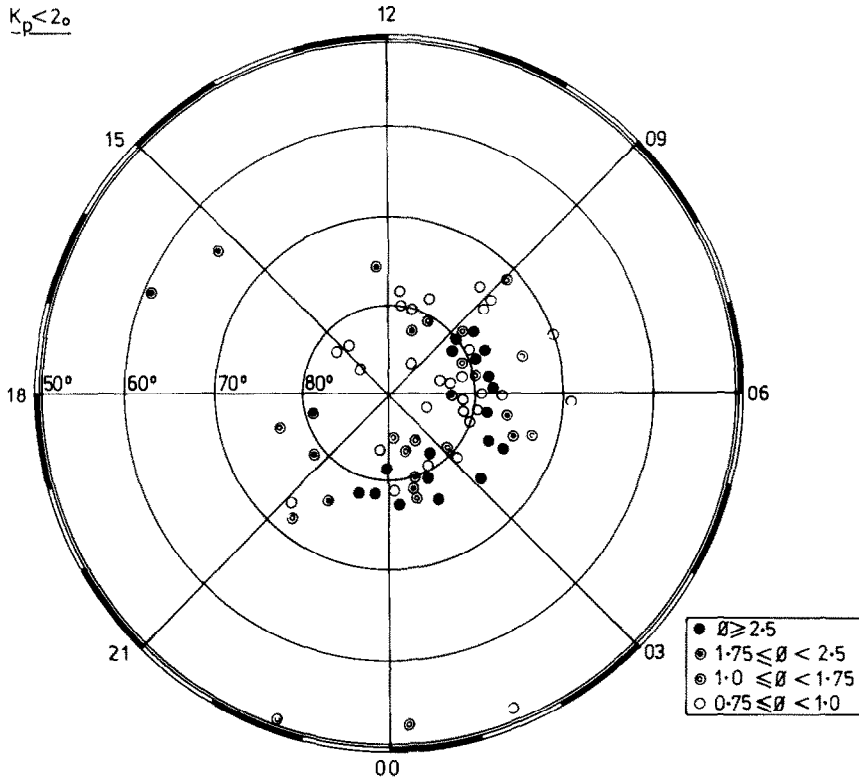


FIG. 9. LOCAL TIME-GEOMAGNETIC LATITUDE PLOT OF OBSERVATIONS OF θ IN VARIOUS RANGES (IN $10^{13} \text{ m}^{-2} \text{ s}^{-1}$) FOR SUMMER AND WINTER WHEN $K_p < 2.0$.

the fraction of the total number of observations which give a flux value exceeding $0.75 \times 10^{13} \text{ m}^{-2} \text{ s}^{-1}$ and shown here for bins of 4 h local time and 10 degrees of latitude. Neither observations for which χ falls in the range 90 – 110° , nor those yielding a profile of the kind shown in Fig. 1, are included in either total and no values are given for bins for which the number of observations does not exceed 20. The occurrence frequency is highest in the 70 – 80° range for winter nights, with lower values at latitudes above 80° . The probability of θ exceeding $0.75 \times 10^{13} \text{ m}^{-2} \text{ s}^{-1}$ can be as high as 0.5, falling to 0.2 for $\theta > 1.75 \times 10^{13} \text{ m}^{-2} \text{ s}^{-1}$. During the summer the probabilities are generally considerably lower, with most events being clustered around the vicinity of the dayside cleft.

The dependence of the occurrence probability on the K_p value is given in Fig. 12, which shows n , the percentage of observations in a given K_p bin yielding a value of θ in one of three ranges. The probability of occurrence increases with K_p for the lower two flux ranges, however for $\theta > 2.5 \times 10^{13} \text{ m}^{-2} \text{ s}^{-1}$ most events occur at very low K_p .

The values of θ are deduced by making use of MSIS predictions of neutral density and temperature. The errors quoted for the model give the maximum errors α_n and α_t in Fig. 4, which, by definition, are not sufficiently large to explain the large θ events. However, it is important to ensure that these events do not arise from errors in the MSIS values which are larger than those quoted. An over-estimate of θ may arise from an under-estimate of the neutral temperature, however θ is only weakly dependent on this parameter (Fig. 4) and errors of several hundred per cent are required to explain any of the events. For most cases the largest error in θ arises from the neutral density, N_o ; as θ is proportional to the ionised fraction (N_{o+}/N_o) an underestimate of this parameter would give over-estimates of both (N_{o+}/N_o) and θ . Hence, if exceptionally large errors in the MSIS prediction are a cause of the large θ values then they should arise from a proportionally large (N_{o+}/N_o). This is shown not to be the case by Fig. 13, a scatter plot of θ , deduced from observations poleward of 65° , as a function

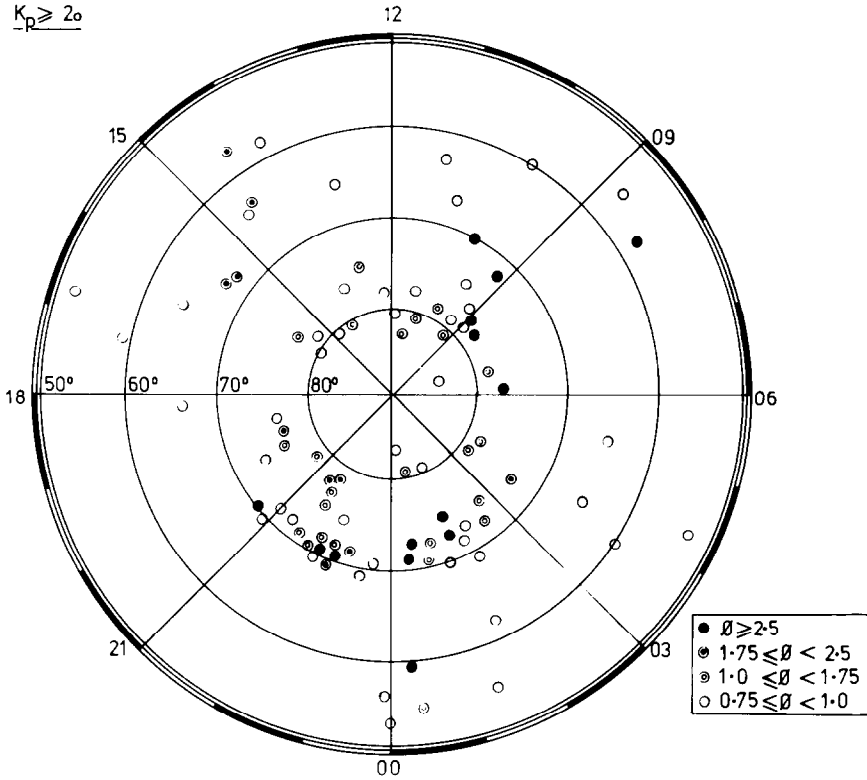


FIG. 10. LOCAL TIME-GEOMAGNETIC LATITUDE PLOT OF OBSERVATIONS OF θ IN VARIOUS RANGES (IN $10^{13} \text{ m}^{-2} \text{ s}^{-1}$) FOR SUMMER AND WINTER WHEN $K_p \geq 2.0$.

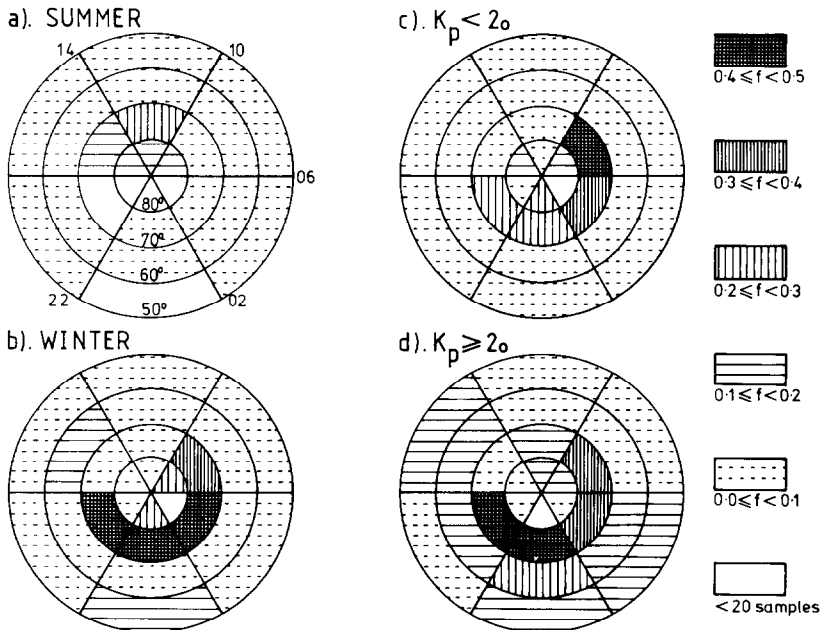


FIG. 11. OCCURRENCE PROBABILITIES OF EVENTS OF $\theta > 0.75 \times 10^{13} \text{ m}^{-2} \text{ s}^{-1}$, f , IN VARIOUS LOCAL TIME-GEOMAGNETIC LATITUDE BINS FOR (a) SUMMER; (b) WINTER; (c) $K_p < 2.0$ AND (d) $K_p \geq 2.0$.

of the ionised fraction. The open circles indicate observations for which the predicted neutral temperature, T_n , is less than 800 K, the solid circles being for all higher neutral temperatures. The ranges of θ used in Figs. 7–10 are shown at the top of the plot, using the same symbols as previously. Higher values of the ionised fraction (> 0.002) do give rise to a few large values of θ , mainly in the lower three ranges of Figs. 7–10. These are always for the higher neutral temperatures and account for most of the observations around the summer cleft in Fig. 8. However, fluxes of all magnitudes are found at lower ionised fractions (< 0.001) and most of the solid points in Figs. 7–10 arise from low ionised fractions and low neutral temperatures, the majority being for winter night conditions (Fig. 7). Hence, although error in the predicted value of N_0 may introduce a similar fractional error in θ , the largest values of θ do not occur for high ionised fractions and hence are very unlikely to be due to excessively low predicted values for N_0 .

4. COMPARISON WITH OBSERVATIONS OF UFI EVENTS

The occurrence of these large upward flow events shows many similarities to that of UFI events as observed by the S3–3 and ISIS satellites. Transversely accelerated ions were frequently observed at 1400 km by ISIS 2 in a broad range of latitudes around the auroral oval (Ungstrup *et al.*, 1979). Klumpar (1979) has studied the occurrence frequency of such ions and found that peak values were between 0.3 and 0.6, for latitudes in the range 65–75° on winter nights between 21 and 06 hours L.T., in agreement with Fig. 11. Also very few UFI events were observed during summer by ISIS 2, however at greater altitudes (> 2750 km) ISIS 1 detected some in the region of the cleft. Hence the acceleration here must occur at some altitude above ISIS 2, where it cannot act as a source of O^+ . This is consistent with the lower O^+ ion flux observed in the magnetotail for the mantle than for the more central lobes and plasma sheet (Sharp *et al.*, 1981).

Ghielmetti *et al.* (1978) studied the latitudinal, diurnal and altitudinal morphology of UFI events including both beams and conics of both ion species. The occurrence of such events, detected by the S3–3 ion mass spectrometer, was found to peak in the auroral oval, with a few events at invariant latitudes greater than 85° but none below 60°. The probability of observation was 0.3 near the satellite apogee (8000 km), falling to zero for altitudes below 3000 km. In addition, few events were

detected after local midnight, in contrast with Fig. 11. The ion mass spectrometer does not detect ions with energies below 500 eV, which weighs the study in favour of beams, which are more energetic in general. Gorney *et al.* (1981) have distinguished between beams and conics, and find the morphology described by Ghielmetti *et al.* does indeed resemble that of ion beams.

Using the S3–3 electrostatic ion analyser, which has a detection threshold of 90 eV, Kintner *et al.* (1979) found the probability of observing an UFI event to be 0.4 between 2000 and 4000 km altitude and 0.1 below 2000 km. Gorney *et al.* (1981) also have used this instrument to study the morphology of beams and conics separately, but without mass resolution. The vast majority of conics are found in their lowest energy range of 90–400 eV.

The probability of observations has a constant value of 0.1 down to 1000 km for $K_p < 3$, and increases to 0.1 with decreasing altitude below 2000 km for $K_p > 3$. These occurrence frequencies are somewhat lower than those given in Fig. 11, but represent means over all local times and all altitudes above 58° for a period between July and December. The low energy, low altitude conics are thought to be O^+ ions, but are found considerably less frequently than the low energy conics observed at 1400 km (Klumpar, 1979). The energy threshold for the latter ISIS 2 observations is 5 eV, whereas the S3–3 ESA only detects energies down to 90 eV, hence conics of energy between these two thresholds can explain the difference in occurrence probabilities. Given the threshold for O^+ escape is about 10 eV (Moore, 1981), the frequency of thermal O^+ flow events should, if they are associated with low altitude conic generation, be closer to the values found by Klumpar than those found by Gorney *et al.* (1981). Figure 11 shows that, in general, this is the case.

The major difference between the morphology of large upward fluxes of thermal ions and that of low energy conics observed by Klumpar and Gorney *et al.*, is the smaller probability of occurrence within the auroral oval itself. However, it must be remembered that many topside soundings in this region were discarded because effects of transient ion production in the F layer were detected, the interpretation of such observations being ambiguous. Another complication in the auroral region is the rapid convective motion of plasma on the night side towards dawn. Schunk *et al.* (1976) have used a full time-dependent model to determine the evolution of the topside F layer profile under model increases in electric field, both

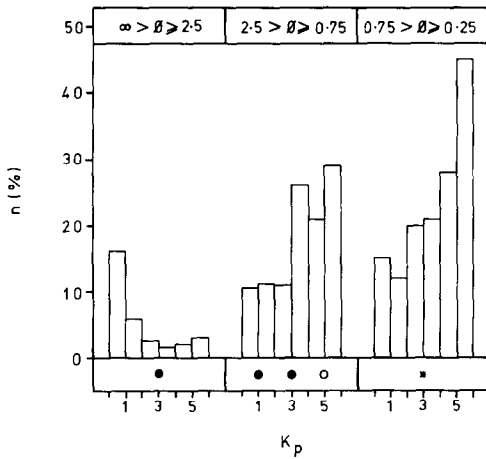


FIG. 12. n , THE PERCENTAGE OF OBSERVATIONS POLEWARD OF 65° IN A GIVEN K_p BIN, GIVING VALUES OF θ IN ONE OF THREE RANGES (IN $10^{13} \text{ m}^{-2} \text{ s}^{-1}$).

with and without polar wind outflow. In some of their examples the signature in the scale height profile which is calibrated here (Fig. 3) is altered by the enhanced horizontal motion. However, the effect is much smaller than that due to an ion outflow, and the error in the deduced flux is small.

Given that either of the above effects may have somewhat reduced probabilities within the auroral oval, the occurrence shown in Fig. 11 for $K_p > 2$ shows a striking similarity to the local time-latitude occurrence of conics observed by the S3-3 ESA when K_p exceeded 3 (Gorney *et al.*, 1981). For the lower K_p values, however, the agreement is not so close, there being a higher probability of observing a conic after, as opposed to before, local midday. Sharp *et al.* (1981) have observed streams of O^+ in the magnetotail using the ISEE 1 ion mass spectrometer. At low K_p ($< 3^+$) such streams are observed as frequently in the tail lobes as in the plasma sheet (occurrence frequencies 0.1 for energies per charge of 110 eV to 17 keV above spacecraft potential), implying an ionospheric source active within both the polar cap and the auroral oval. At higher magnetic activities ($K_p > 4^-$) the flows are found with twice this frequency in the lobes whereas the probability exceeds 0.45 in the plasma sheet, so the peak of the ionospheric source moves more equatorward during magnetic activity than does the auroral oval itself. Figures 9 and 10 show that large flux events occur at higher latitudes, relative to the auroral oval, for the lower K_p values. The same behaviour can be seen in the

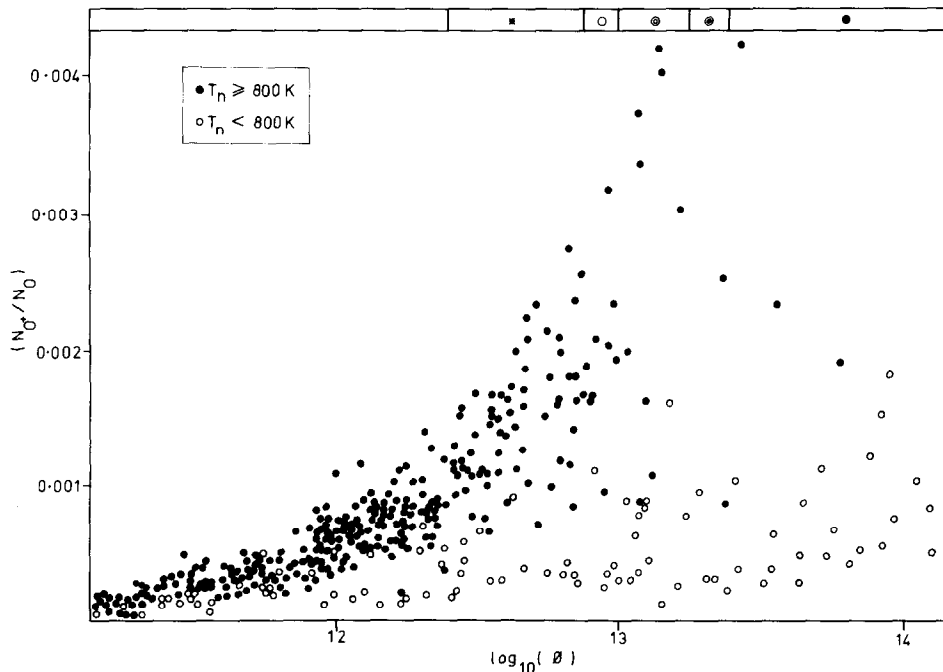


FIG. 13. SCATTER PLOT OF $\log_{10}(\theta)$, WHERE θ IS IN $\text{m}^{-2} \text{ s}^{-1}$, AS A FUNCTION OF IONISED FRACTION, N_{o^+}/N_o , FOR ALL OBSERVATIONS POLEWARD OF 65° , GEOMAGNETIC.

Open points are for predicted neutral temperature, T_n , less than 800 K; solid points are for all greater T_n .

equinoctial mean flux values given in Figs. 2 and 3 of Lockwood and Titheridge (1981). Given that the number of events within the oval may have been reduced by the effects described previously, the large O^+ flows therefore behave in the way expected for the source of the magnetotail streams.

5. DISCUSSION

The similarities listed in the previous section provide an indication that the events of large upward flux of thermal O^+ may be connected with the generation of low energy O^+ conics. Hence it is worth considering the possible effects of such heating on the dynamics of the thermal ion population. The satellite observations give no resolution of the temporal and spatial variations of the regions of transverse O^+ acceleration. However, it is unlikely that the heating is present for sufficient time for steady state conditions to become established. If steady state did apply θ would equal the total ion flux entering the magnetosphere, however the magnitudes of θ observed (Fig. 13) are often considerably larger than is required to both support the polar wind and act as a source of beams and conics. Bering *et al.* (1975) detected flows of thermal plasma below 500 km, beneath a region of transverse O^+ acceleration, during a rocket flight. The flow was downward indicating an expansion away from a localised "hot spot" which was thought to be due to oxygen cyclotron wave heating. In less intense heating events, this effect would simply reduce the upward flow required to support the polar wind, and hence would not be identified in this study. When the heating ceases (either because the field-aligned current density falls below the instability threshold, or because the plasma has convected out of the heating region) the hot spot will cool and become a localised hole in the plasma, depleted by the thermal expansion and by the upward motion of the energised ions by the gradient B force. Large refilling O^+ fluxes would then be able to flow upward, unlimited by charge exchange with neutral hydrogen. Hence, the large θ events would be due to the cessation of transverse acceleration at altitudes above the observation but below the O/H neutral transition altitude. If the depletion is mainly due to the loss of energised ions to the magnetosphere then the large θ events will correspond, not to the more intense heating events, but to the more long-lived ones. This may be an explanation of the K_p dependence shown in Fig. 12, in that there is an increase in occurrence of transverse heating events with

magnetic activity, as observed at low altitudes by Gorney *et al.* (1981), but the enhanced convection results in fewer long-lived heating events, and hence fewer of the largest θ events.

Cattell *et al.* (1979) report conics in all regions of field-aligned current, of both senses. Figures 7–10 show that although large θ events occur in regions where field-aligned currents would be expected (Akasofu *et al.*, 1980), not all such regions give events. From their locations large θ events would appear to occur predominantly in the region of downward current which extends in local time from about 22–10 h. As has been discussed previously, the small number of events in the equatorward of the regions of field-aligned current may be due to the elimination of profiles showing the effects of F layer production by particle precipitation. This does not, however, explain the near complete absence of events from the poleward region of upward current around dusk. Such current would predominantly be carried by precipitating magnetospheric electrons. Dusenbery and Lyons (1982) have found that these electrons should not give ion cyclotron wave heating of O^+ , because their energy is too high. Hence, conics should only be generated in regions of downward current, which are predominantly carried by upstreaming low-energy ionospheric electrons. This is therefore consistent with the morphology of large θ events shown Figs. 7–11, and is also indicated by the study of conics by Cattell (1981).

The largest values deduced for θ require differences in the field-aligned velocities of O^+ ions and O atoms of up to about 1 km s^{-1} (by equation 1). Fabry–Perot observations at Spitsbergen by Smith (private communication) in January 1981 give an example of a velocity of O^+ ions vertically upward of this order of magnitude, with no response in the neutral atmosphere motion. The magnetic field is at an angle of 7° to the vertical, hence it is unlikely that the effect can be due to field-perpendicular motions and in this case a large value of θ would have been observed by the topside sounder.

6. CONCLUSIONS

Upward field aligned flows of O^+ in the topside auroral ionosphere are found often to be significantly larger than is required for support of the light ion polar wind. Many of these cases can be explained as being, at least in part, due to enhanced ion production, either by particle precipitation or by convection into the sunlit hemisphere. However, the remaining events appear to

constitute a violation of charge exchange chemistry unless a low-altitude transverse heating mechanism is invoked. Such heating would be a source of O^+ conics and the occurrence of the remaining large flow events does indeed bear many similarities to that of low energy conics. The differences can be understood by considering the energy thresholds of the various transversely accelerated ion detectors, and the expected threshold for escape of O^+ by ion-cyclotron heating. Other differences can be explained in terms of the analysis required to define unambiguously an event of large O^+ flow. Oxygen cyclotron waves are expected to be present at sufficiently low altitudes in regions of downward field-aligned current, and consideration of their effects on the thermal plasma suggests that a localised depletion may be formed. On removal of the heating O^+ ions would then flow upward from beneath, unrestricted by charge exchange with neutral hydrogen. Hence the flux magnitudes are large and are a larger fraction of the limiting value set by ion-neutral frictional drag. The transversely accelerated ions are moved upward by the magnetic field gradient, and act as a source of the ionospheric O^+ found in various parts of the magnetosphere.

Acknowledgements—Initial research for this work was carried out at the Communications Research Centre, Ottawa, by Dr J. E. Titheridge, to whom I am greatly indebted. I am also grateful to the Auckland University Council for the award of a Postdoctoral Research Fellowship, and to Dr H. Rishbeth for valuable discussion and helpful comments, and to Dr R. Smith for supplying the Fabry-Perot observations.

REFERENCES

- Akasofu, S. I., Ahn, Bynug-Ho and Kisabeth, J. (1980). Distribution of field-aligned currents and expected magnetic field perturbations resulting from auroral currents along circular orbits of satellites. *J. geophys. Res.* **85**, 6883.
- Ashour-Abdalla, M., Okuda, H. and Cheng, C. Z. (1981). Acceleration of heavy ions on auroral field lines. *Geophys. Res. Lett.* **8**, 795.
- Banks, P. M. and Holzer, T. E. (1969). High latitude plasma transport: the polar wind. *J. geophys. Res.* **74**, 6317.
- Bering, E. A., Kelley, M. C. and Mozer, F. S. (1975). Observations of an intense field-aligned thermal ion flow and associated intense narrow band electric field oscillations. *J. geophys. Res.* **80**, 4612.
- Cattell, C. A. (1981). The relationship of field-aligned currents to electrostatic ion cyclotron waves. *J. geophys. Res.* **86**, 3641.
- Cattell, C. A., Lysak, R. L., Torbert, R. B. and Mozer, F. S. (1979). Observations of differences between regions of current flowing into and out of the ionosphere. *Geophys. Res. Lett.* **6**, 621.
- Croley, D. R., Jr, Mizera, P. F. and Fennell, J. F. (1978). Signature of parallel electric field in ion and electron distributions in velocity space. *J. geophys. Res.* **83**, 2701.
- Dusenbery, P. B. and Lyons, L. R. (1982). Generation of ion-conic distributions by upgoing ionospheric electrons. *J. geophys. Res.* **86**, 7627.
- Frank, L. A., Ackerson, K. L. and Yeager, D. M. (1977). Observations of atomic oxygen (O^+) ions in the Earth's magnetotail. *J. geophys. Res.* **82**, 129.
- Ghielmetti, A. G., Johnson, R. G., Sharp, R. D. and Shelley, E. G. (1978). The latitudinal, diurnal and altitudinal distributions of upward flowing energetic ions of ionospheric origin. *Geophys. Res. Lett.* **5**, 59.
- Gorney, D. J., Clarke, A., Croley, D., Fennell, J., Luhmann J. and Mizera, P. (1981). The distribution of ion beams and conics below 8000 km. *J. geophys. Res.* **86**, 83.
- Hoffman, J. H. and Dodson, W. H. (1980). Light ion concentrations and fluxes in polar regions during magnetically quiet times. *J. geophys. Res.* **85**, 626.
- Johnson, R. G. (1979). Energetic ion composition in the Earth's magnetosphere. *Rev. Geophys. Space Phys.* **17**, 696.
- Kindel, J. M. and Kennel, C. F. (1971). Topside current instabilities. *J. geophys. Res.* **76**, 3055.
- Kintner, P. M., Kelley, M. C., Sharp, R. D., Ghielmetti, A. G., Temerin, M., Cattell, C., Mizera, P. and Fennell, J. F. (1979). Simultaneous observations of energetic (keV) upstreaming and electrostatic hydrogen cyclotron waves. *J. geophys. Res.* **84**, 7201.
- Klumpar, D. M. (1979). Traversely accelerated ions: an ionospheric source of hot magnetospheric ions. *J. geophys. Res.* **84**, 4229.
- Lockwood, M. and Titheridge, J. E., (1981). Ionospheric origin of magnetospheric O^+ ions. *Geophys. Res. Lett.* **8**, 381.
- Lockwood, M. and Titheridge, J. E. (1982). Departures from diffusive equilibrium in the topside F layer from satellite soundings. *J. atmos. terr. Phys.* **44**, 425.
- Lockwood, M. (1982). Field-aligned plasma flow in the quiet, mid-latitude ionosphere deduced from topside soundings. *J. atmos. terr. Phys.* (submitted).
- Lysak, R. L., Hudson, M. K. and Temerin, M. (1980). Ion heating by strong electrostatic ion cyclotron turbulence. *J. geophys. Res.* **85**, 678.
- Moore, T. E. (1980). Modulation of terrestrial ion escape flux composition (by low altitude acceleration and charge exchange chemistry). *J. geophys. Res.* **85**, 2011.
- Mozer, F. S., Cattell, C. A., Hudson, M. K., Lysak, R. L., Temerin, M. and Torbert, R. B. (1980). Satellite measurements and theories of low altitude auroral particle acceleration. *Space Sci. Rev.* **27**, 155.
- Palmadesso, P. J., Coffey, T. P., Ossakow, S. L. and Papadopoulos, K. (1974). Topside ionosphere ion heating due to electrostatic ion cyclotron turbulence. *Geophys. Res. Lett.* **1**, 105.
- Papadopoulos, K., Gaffey, J. D., Jr. and Palmadesso, P. J. (1980). Stochastic acceleration of large M/Q ions by hydrogen cyclotron waves in the magnetosphere. *Geophys. Res. Lett.* **7**, 1014.
- Prange, R. (1978). Energetic (keV) ions of ionospheric origin in the magnetosphere. A review. *Annlis Géophys.* **34**, 187.

- Schunk, R. W., Banks, P. M. and Raitt, W. J. (1976). Effects of electric fields and other processes upon the night-time high-latitude *F* layer. *J. geophys. Res.* **81**, 3271.
- Sharp, R. D., Carr, D. L., Peterson, W. K. and Shelley, E. G. (1981). Ion streams in the magnetotail. *J. geophys. Res.* **86**, 4639.
- Titheridge, J. E. (1976). Ion transition heights from topside electron density profiles. *Planet. Space. Sci.* **24**, 229.
- Ungstrup, E., Klumpar, D. M. and Heikkila, W. J. (1979). Heating of ions to superthermal energies in the topside ionosphere by electrostatic ion cyclotron waves. *J. geophys. Res.* **84**, 4289.
- Whalen, B. A., Bernstein, W. and Daly, P. W. (1978). Low altitude acceleration of ionospheric ions. *Geophys. Res. Lett.* **5**, 55.
- Whittaker, J. H. (1977). The transient response of the topside ionosphere to precipitation. *Planet. Space Sci.* **25**, 773.
- Reference is also made to the following unpublished material:
- Brinton, H. C. and Grebowsky, J. M. (1978). AE-C observations of upward-streaming O^+ ions, Atmospheric Explorer Symposium, Bryce Mountain Resort, October 1978.